



Vibrational spectra and density functional theoretical calculations on the NLO crystal DL-Valinium trifluoroacetate

D Manimaran^a, I Hubert Joe^{a*}, Daisy Bhat^b and V K Rastogi^{b,c}

^aCentre for Molecular and Biophysics Research, Department of Physics, Mar Ivanios College, Thiruvananthapuram-695 015, India.

^bR D Foundation Group of Institutions, NH-58, Kadrabad (Modinagar), Ghaziabad, India

^cIndian spectroscopy society, K.C 68/1, Old Kavi Nagar, Ghaziabad- 201 002, U.P, India.

Good optical quality single crystal of DL-Valinium trifluoroacetate (VLTFa) was grown by slow evaporation technique. The grown crystal was characterized by FT-IR and FT-Raman spectra and analyzed. The DFT computations were performed at B3LYP level with 6-31G(d,p) basis set to derive molecular structural parameters, vibrational wavenumbers, intensities, atomic charges distribution of VLTFa molecule. Vibrational analysis was used to investigate O-H...O=C and N-H...O=C hydrogen bonding interactions. Mulliken population analysis, hyperpolarizability and HOMO-LUMO energy gap are calculated by density functional theory. © Anita Publications. All rights reserved.

1 Introduction

Nonlinear optical (NLO) materials, defined as materials in which light waves can interact with each other, are the key materials for the fast processing of information and for dynamic or permanent optical storage applications[1]. The design of nonlinear optical molecules has become a focus of current research in view of their potential applications in various photonic technologies. Synthesis[2-6], theoretical[7-9] and spectroscopic[10-12] studies of amino acid derivatives NLO crystals were reported by several authors. DL-Valinium trifluoroacetate crystal first synthesized and reported by Suresh *et al.*[13]. VLTFa crystallizes in triclinic space group P_1 and $Z = 2$. The unit cell parameters were $a = 6.7282(6) \text{ \AA}$; $b = 9.0830(4) \text{ \AA}$; $c = 9.2148(7) \text{ \AA}$. DL-Valinium trifluoroacetate ($C_5H_{12}NO_2^+ \cdot C_2F_3O_2^-$) is one of the most attractive compound in the L-Valinine family. We have tried to grow single crystals of VLTFa for the study the hydrogen bonding features with aid of vibrational spectral technique. The present work describes the vibrational spectral investigations aided by density functional theory computations to elucidate the correlation between the molecules structure, hydrogen bonding features and NLO property investigating of the VLTFa crystal

2 Experimental and computational details

2.1 Synthesis and characterization

The compound DL-Valine (99%) and Trifluoroacetic acid (99%) were purchased from Sigma-Aldrich Company. DL-Valine and Trifluoroacetic acid were taken in 1:1 stoichiometric ratio in deionized double distilled water to get saturated aqueous solution and was then allowed to evaporate slowly at room temperature. Good quality transparent single crystals of LARPCL were obtained within two weeks, twice recrystallization yielded good quality crystals. The grown VLTFa crystals were characterized by FT-IR (400-4000 cm^{-1}), NIR FT-Raman (50-3500 cm^{-1}) spectroscopic technique.

Corresponding author :

e-mail: hubertjoe@gmail.com (Dr I Hubert Joe)

2.2 Molecular orbital calculations

Density functional theory calculations were performed at the Becke three [14] exchange functional in combination with both the correlational functional of Lee, Yang and Parr (LYP) [15] level with 6-31G(d,p) basis set using Gaussian 09 program package [16]. Calculated vibrational frequencies were uniformly scaled by 0.961 [17] in order to neglect systematic errors by basis set incompleteness, electron correlation and harmonicity. The calculated Raman activities have been converted to relative Raman intensities from the intensity theory of Raman scattering [18,19]. The simulated IR and Raman spectra have been plotted using pure Lorentzian band shape of 10 cm⁻¹ fwhm.

The first order hyperpolarizability was calculated using B3LYP/6-31G(d,p) level basis set on the basis of the finite-field approach. The components of the first order hyperpolarizability can be calculated using the following equation:

$$\beta_i = \beta_{iii} + 1/3 \sum (\beta_{ijj} + \beta_{jij} + \beta_{jji}), (i \neq j) \quad \dots (1)$$

Using the x, y and z components, the magnitude of the first order hyperpolarizability tensor can be calculated by

$$\beta_{tot} = (\beta_x^2 + \beta_y^2 + \beta_z^2)^{1/2} \quad \dots (2)$$

The complete equation for calculating the magnitude of first order hyperpolarizability from Gaussian 09 output is given as follows:

$$\beta = [(\beta_{xxx} + \beta_{xyy} + \beta_{xzz})^2 + (\beta_{yyy} + \beta_{yzz} + \beta_{yxx})^2 + (\beta_{zzz} + \beta_{zxx} + \beta_{zyy})^2]^{1/2} \quad \dots (3)$$

The calculated first order hyperpolarizability of VLTFa was found to be 6.42×10^{-30} e.s.u, which is 25 times that of urea. This greater 'β' value reflects the high NLO efficiency of VLTFa crystal.

3. Result and Discussion

3.1 Molecular Geometry

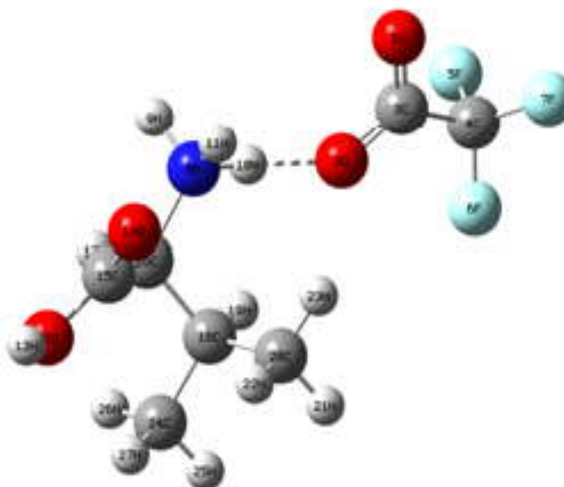


Fig. 1 Optimized structure of DL-Valinium trifluoroacetate (VLTFa)

The optimized structure with atom numbering scheme of VLTFa is shown in Fig. 1 while the corresponding structural parameters combined with experimental data [13] are listed in Table 1. From the structural geometry, O-H calculated bond length (0.9754 Å) is longer than the experiment (0.820 Å) data, this deviations

in values indicates the formations of O-H \cdots O hydrogen bonding in the crystalline state. Similarly, N-H experimental bond lengths are significantly less than the computed values; this deviations occurs influence of inter and intra molecular (N-H \cdots O) hydrogen bonding interactions. C₁₅-C₁₆-O₁₂(H₁₃), C₁₅-C₁₆=O₁₄ bond angles are found to be 112.66° and 121.43° respectively. These deviations in geometrical parameters are due to influence of O-H \cdots O hydrogen bonding formation in crystalline surface. The N₈-(H) \cdots O₂ (2.9 Å) distance is significantly shorter than the van der Waals separation between O and H atom indicates the possibility of N-H \cdots O hydrogen bonding. Bond angle of N₈-H₁₀ \cdots O₂ is calculated to be 176.37° (it nearby 180°) the result supports the intramolecular charge transfer (ITC) interaction lie between these hydrogen bonding donor and acceptor moiety. The DFT level calculated structural parameters were in agreement with the XRD results.

Table 1. Optimized parameters of VLTFa by B3LYP level with 6-31G(d,p) basis set

Bond length	Values (Å)		Bond angle	Values (°)		Dihedral angle	Values (°)	
	Calc.	Exp. ^a		Cal.	Exp. ^a		Cal.	Exp. ^a
O1-C3	271	1.225	C3-O2-H10	134.94	105.81	H10-O2-C3-C4	157.32	166.64
O2-C3	1.2454	1.231	O1-C3-O2	114.69	124.97	O2-C3-C4-F5	33.43	-40.36
O2-H10	1.8634	1.969	O2-C3-C4	123.98	117.24	O2-C3-C4-F6	-85.27	87.92
C3-C4	543	1.507	C3-C4-F5	108.45	113.96	O2-C3-C4-F7	154.18	-157.30
C4-F5	1.3348	1.300	C3-C4-F6	108.73	117.48	H10-N8-C16-C18	56.57	-179.97
C4-F6	1.3318	1.306	C3-C4-F7	109.31	106.89	C16-C18-C24-H25	172.72	179.94
C4-F7	1.3309	1.348	F5-C4-F6	109.76	108.35	C16-C18-C24-H26	53.93	60.00
N8-H9	1.0235	0.890	C18-C20-H21	109.4	109.44	C16-C18-C24-H27	-67.7	-60.05
N8-H10	1.0369	0.891	C18-C20-H22	111.79	109.47	C16-C18-C20-H21	-174.7	179.99
N8-H11	1.0366	0.890	H22-C20-H23	106.81	109.43	C16-C18-C20-H22	66.49	60.05
N8-C16	1.5202	1.486	C16-C18-C20	112.71	112.84	C16-C18-C20-H23	-55.7	-60.03
O12-H13	0.9754	0.820	C16-C18-H19	104.87	106.41	H11-N8-C16-C18	-65.1	-59.98
O12-C15	1.3255	1.300	H9-N8-C16	111.52	109.50	H9-N8-C16-C18	177.9	179.97
O14-C15	1.215	1.203	C15-C16-H17	110.12	108.79	N8-C16-C18-C24	-161.67	-160.44
C15-C16	1.5331	1.516	H10-N8-C16	110.9	109.48	C15-C16-C18-C24	79.65	79.64
C16-H17	1.0924	0.980	H11-N8-C16	106.03	109.50	O14-C15-C16-C18	113.67	106.11
C16-C18	1.5549	1.545	H13-O12-C15	109.00	109.40	O12-C15-C16-C18	-66.91	-72.63
C18-H19	1.0985	0.979	O12-C15-C16	112.66	111.73	H13-O12-C15-C16	-179.67	-176.24
C18-C20	1.5364	1.506	O14-C15-C16	121.43	123.03	O14-C15-C16-H17	-121.37	-132.96
C18-C24	1.5362	1.512	C16-C18-C24	110.96	111.41	C15-C16-C18-H19	-164.73	-164.84
C20-H21	1.0926	0.960	C18-C16-C15	114.43	113.08	C15-C16-C18-C20	-46.59	-48.54
C20-H22	1.0946	0.960	N8-C16-C18	110.67	110.21	H10-O2-C3-O1	-21.02	-14.03
C20-H23	1.0956	0.960	C18-C24-H25	107.99	109.49	H10-N8-C16-C15	-178.06	-56.54
C24-H25	1.0928	0.960	C18-C24-H26	109.1	109.45	C15-C16-C18-C24	74.34	48.54
C24-H26	1.0942	0.960	C18-C24-H27	111.82	109.46	N8-C16-C18-C20	64.43	71.38
C24-H27	1.0923	0.960	N8-H10 \cdots O2	176.37°	161.34	N8-C16-C18-C24	169.05	160.48

^aTaken from [13].

3.2 Vibrational spectral analysis

The vibrational analysis were performed using DFT method B3LYP/6-31G(d,p) level basis set. The calculated vibrational wavenumbers, measured infrared and Raman band positions and their assignments are present in Table 2. The observed FT-IR and FT-Raman spectra of VLTFa are given in Fig. 2 and 3.

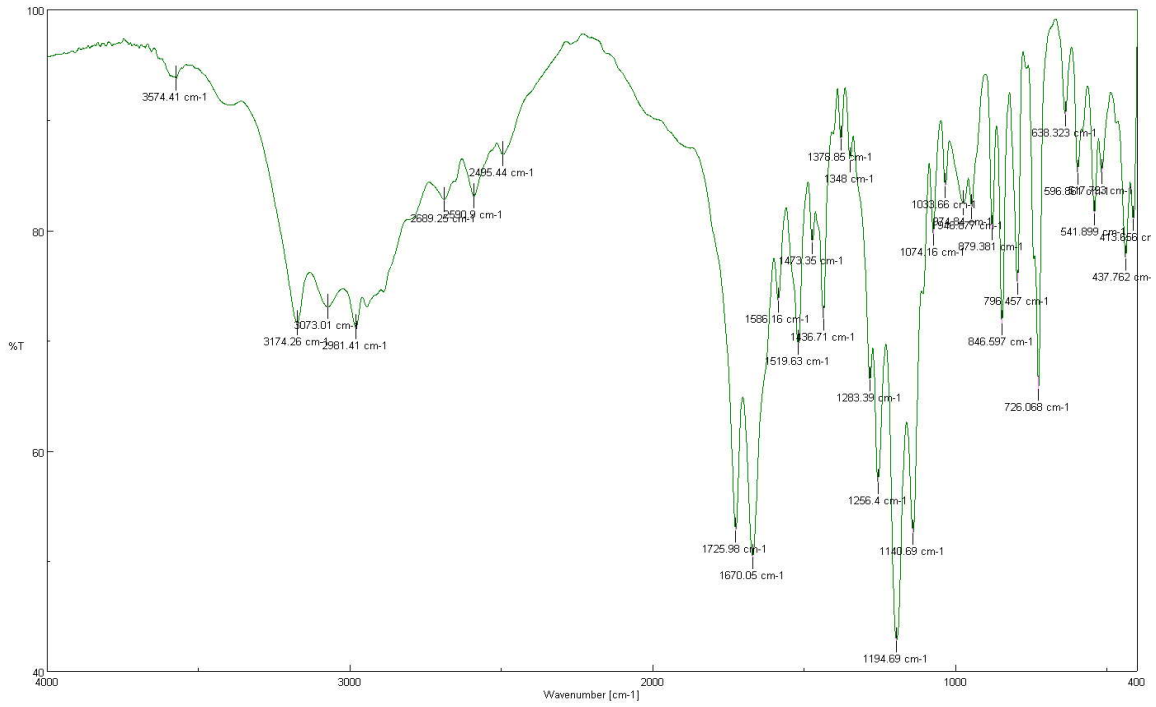


Fig. 2 FT-IR spectrum for DL-Valinium trifluoroacetate

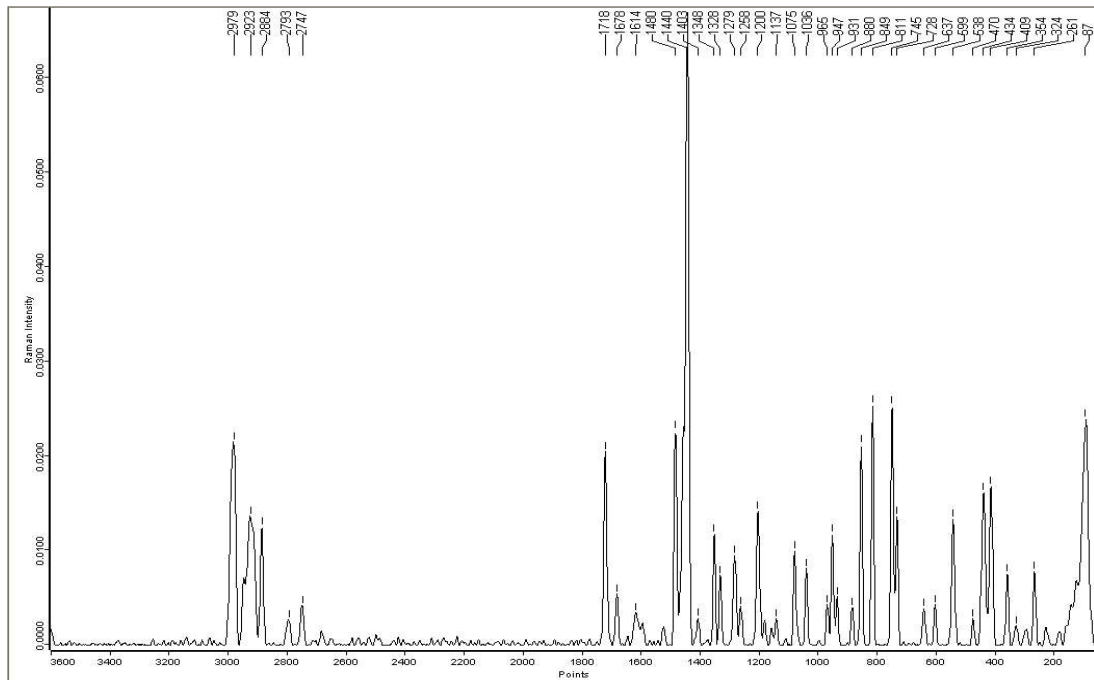


Fig. 3 FT-Raman spectrum for DL-Valinium trifluoroacetate

Table 2: Computed vibrational wavenumbers and fundamental bands positions assignments of VLTA

Calculated Wavenumber (cm ⁻¹)	Experimental wavenumber (cm ⁻¹)		Forces constant (Debye)	Vibrational assignments with PED%
	IR	Raman		
3579	3574 v.w	---	8.70	ν O12-H13 (100)
3360	---	---	7.79	ν N8-H9 (97)
3171	3174 m	---	6.99	ν N8-H10 (19), ν N8-H11 (80)
3108	3073 m. brd.	---	6.47	ν N8-H10 (79), ν N8-H11 (18)
3029	---	---	6.46	ν C24-H25 (30), ν C24-H27 (64)
3019	---	---	6.4	ν C20-H21(73), ν C20-H22 (18)
3014	---	---	6.39	ν C24-H25(41), ν C24-H26 (47)
3002	---	---	6.25	ν C16-H17(99)
2996	2981 m	2979 s	6.31	ν C20-H22(45), ν C20-H23(47)
2944	2940 m	2944 w.shr.	5.74	ν C24-H25(27), ν C24-H26(48), ν C24-H27(24)
2932	---	---	5.7	ν C20-H21(16), ν C20-H22(32) ν C20-H23(50)
2921	---	2923 m	5.9	ν C18-H19 (97)
	2889 m. shr.	2884 m		ν C24-H25(38), ν C24-H27 (34)
	---	2793 v.w		
	---	2747 w.		
	2689 w.brd.	---		
	2591 w	---		Overtones and Combination bands
	2561 w.shr	---		
	2495 w.brd.	---		
1758	1726 s	1718 s	17.43	ν O14-C15 (82)
	1670 s	1678 w		ν C=O
1620		1614 v.w.	1.75	δ H9-N8-H10 (62)
1593	1586 m	1591 v.w	1.71	δ H9-N8-H10 (21), δ H10-N8-H11 (49)
1531	1520 m	1521 v.w	18.21	ν O2-C3(52), ν O1-C3 (26), ν C3-C4 (17)
1464	1473 w	1480 s	1.44	δ H21-C20-H22 (50)
1461	---	---	1.48	δ H10-N8-H11 (11), δ H22-C20-H23 (19), δ H26-C24-H27 (18)
1458	---	1452 s. shr.	1.56	δ N8-H10-O2 (14), δ H10-N8-H11 (22)
1449	---	1440 v s	1.4	δ H21-C20-H22 (25), δ H26-C24-C18 (12)
1434	1437 m	---	1.37	δ H22-C20-H23 (62), δ H26-C24-H27 (15)
1407	---	1403 v.w	2.81	ν O12-C15 (23), ν C15-C16 (12), δ H13-O12-C15 (11), δ O12-C15-O14 (10)
1396	---	---	1.51	δ H25-C24-C18 (15), δ H26-C24-H27 (12)
1374	1378 v.w	---	1.48	δ H25-C24-C18 (24), δ H26-C24-H27 (27)
1324	1348 w	1348 m	1.49	δ H19-C18-C20 (46)
1315	---	1328 w	1.64	ν O12-C15 (10), δ H13-O12-C15 (13)
1293	1283 m	---	1.37	δ H19-C18-C20 (11)
1268	1256 s	1279 w	12.74	ν O2-C3(25), ν O1-C3 (18), ν F6-C4 (14), δ C4-C3-O2(14)
1234	---	1258 v.w	1.58	δ H17-C16-C18 (39), δ H19-C18-C20 (10)
1221	---	---	12.53	ν O2-C3(17), ν O1-C3 (10), ν F7-C4 (46), ν F6-C4 (12)
1204	1195 v.s	1200 m	12.20	ν F5-C4 (54), ν F6-C4 (27)
1165	---	1177 v.w	1.67	δ H26-C24-C18 (13)
1158	---	---	4.05	ν O1-C3 (13), ν F5-C4 (12), ν F6-C4 (12), δ H13-O12-C15 (10)
1155	---	1153 v.w	2.25	ν O12-C15 (18), δ H13-O12-C15 (30)
1142	1141 s	1137 v.w	1.53	ν C18-C24 (16)
1086	1074 w	---	1.11	δ H17-C16-C18 (12), δ H21-C20-C18 (16)
1063	---	1075 m	0.99	δ N8-H10-O2 (24), δ H21-C20-C18 (12), δ H25-C24-C18 (11)
1030	1034 w	1036 w	1.01	ν C18-C20 (14), ν C18-C24 (16)
	975 v.w brd.	965 v.w	---	δ OHO out-of-plane

949	949 w	947 m	1.67	ν C16-C18 (14), ν N8-C16 (39)
934	---	931 w	0.87	ν C18-C24 (17) δ H21-C20-C18 (25), δ H25-C24-C18 (14)
910	---		0.65	δ H26-C24-C18 (35)
895	879 w	880 v.w	1.1	ν C15-C16 (10), ν C18-C24 (18), ν C16-C18 (14), ν N8-C16 (12)
834	847 m	849 s	1.06	ν C15-C16 (34)
771	796 m	811 s	1.24	ν C18-C20 (20)
765	---	745 s	6.32	ν F7-C4 (17), ν F5-C4 (18), ν F6-C4 (17), ν C3-C4 (23)
702	726 m	728 s	0.93	ν C16-C18 (17), δ O12-C15-O14 (11),
701	---	---	3.14	δ O1-C3-O2 (26)
644	638 v.w.	637 m	0.52	δ O12-C15-O14 (27), τ H13-O12-C15-C16 (38)
596	597 w	599 v.w	0.45	δ O12-C15-O14 (12), τ H13-O12-C15-C16 (42)
584	---	---	3.41	ν O1-C3 (16), δ F5-C4-F7 (14), δ C4-C3-O2 (31)
552	542 w	538 v.w	3.13	δ C4-C3-O1 (19), δ F5-C4-F6 (26)
495	518 w	---	0.59	ν C16-C18 (10), ν N8-C16 (17), δ O12-C15-O14 (16)
478	---	470 m	2.52	δ F6-C4-F7 (51), δ F5-C4-F7 (22)
442	438 w	434 v.w	0.33	τ C18-C16-C20-C24 (37)
415	414 w	409 m	0.86	δ F5-C4-F7 (24), δ F5-C4-F6 (13), δ C4-C3-O2 (15)
400	---	---	0.39	δ C16-C18-C20 (10), δ C18-C16-N8 (25)
352	---	354 s	0.64	ν C3-C4 (20), δ C4-C3-O1 (24), δ F5-C4-F6 (17)
331	---	---	0.19	δ C20-C18-C24 (60)
320	---	324 v.w	0.26	δ C16-C15-O12 (46)
299	---	290 v.w	0.06	δ H10-N8-H11 (11), δ H9-N8-H11 (22)
244	---	261 v.w	0.09	δ C16-C18-C20 (38)
229	---		0.04	τ H23-C20-C18-C24 (32)
219	---	223 v.w	0.06	τ H23-C20-C18-C24 (28)
218	---	--	0.08	τ H23-C20-C18-C24 (20)
193	---	---	0.35	δ C4-C3-O1 (35), δ C4-C3-O2 (11)
171	---	138 v.w.shr.	0.06	δ C15-C16-C18 (46)
108	---	120 w.shr.	0.03	ν O2-N8 (15)
89	---	87 s	0.03	ν O2-N8 (55)
59	---	---	0.01	δ C3-O2-N8 (16) δ C16-N8-O2 (29)
59	---	---	0.01	δ C16-N8-O2 (24)
46	---	---	0.01	τ C20-C18-C16-N8 (12)
23	---	---	0.003	τ C18-C16-N8-O2 (29)
21	---	---	0.002	δ C3-O2-N8 (50), δ C16-N8-O2 (21)
17	---	---	0.001	τ O2-C3-C4-F7 (15)
15	--	----	0.001	τ C18-C16-N8-O2 (36), δ C3-O2-N8 (16)

ν -stretching; δ -bending; τ -torsion; ν -very; s-strong; v.w-very weak; shr.-shoulder; m-medium.

3.2.1 Carboxyl group vibrations

Carboxyl absorptions are sensitive to both chemical and physics effects of the molecule [20]. A weak broad band is observed at 3574 cm^{-1} in IR which corresponds to O-H stretching vibration. Thus it may be inferred that this broad OH band is indeed of O-H \cdots O hydrogen bonding in the crystal system. When the carboxyl C=O indicates the hydrogen-bonded, but not dimerized as in alcohol-carbonyl bonding; a band is seen near 1730-1705 cm^{-1} in both IR and Raman [21,22]. The C=O vibrations observed as a strong bands at 1726 and 1718 cm^{-1} in both IR and Raman respectively. The partial bonds of CO stretching vibrations are observed at 1520 cm^{-1} in IR and 1521 cm^{-1} in Raman, the corresponding calculated wavenumber at 1531 cm^{-1} with 52% PED. This results supports carboxylic acid doesn't exists as a dimer in VLFTA crystal. Two bands are observed at 1403 cm^{-1} (Raman) and 1328 cm^{-1} (Raman) both involve interacting is assigned as CO stretch and COH deformations vibrations. Some broad features bands are appears (2690, 2591 and 2496 cm^{-1}) as superim-

posed position of OH stretching band-upon CH stretching vibrations. Combinations of CO and FC stretching vibrations are observed at 1256 cm^{-1} (strong) in IR and 1258 cm^{-1} (weak) in Raman. Carboxylic acid deformations usually appear at $960\text{--}875\text{ cm}^{-1}$ region [22,23]. In VLFTA crystal, IR band is obtained at 975 cm^{-1} (weak broad) and 965 cm^{-1} in Raman as attributed to carboxylic acid deformations. This band noticeably broader (in IR spectrum) than the other bands. This increase wavenumbers indicates the formations of intermolecular hydrogen bonding in crystalline surface.

3.2.2 CF_3 vibrations

C-F stretching vibrations generally appear from $1300\text{--}1000\text{ cm}^{-1}$ [24]. In the present case, a most intense band is observed at 1195 cm^{-1} in IR and a medium band at 1200 cm^{-1} in Raman which is correspond to F-C asymmetric stretching. Similarly, the symmetric stretching F-C vibration is observed as a strong band is observed at 745 cm^{-1} in Raman. CF_3 deformation vibrations is observed as a medium at 470 cm^{-1} in Raman and 414 cm^{-1} (IR), 409 cm^{-1} (Raman) corresponds to in-plane and out-of-plane bending modes respectively. While, CF_3 deformations modes were assigned theoretical predicted at 478 cm^{-1} (scissoring) and 415 cm^{-1} (twisting). The good agreement was found between theoretical and experimental wavenumbers.

3.2.3 NH_3^+ group vibrations

The protonation of NH_3^+ ions stretching vibrations is appears between $3300\text{--}3100\text{ cm}^{-1}$ and $3100\text{--}3000\text{ cm}^{-1}$ for asymmetric and symmetric respectively [25]. The observed bands at 3174 cm^{-1} (asymmetric) and as a medium board band at 3073 cm^{-1} (symmetric) in IR corresponds to NH_3^+ stretching vibrations. The board band indicates to involve of N-H \cdots O hydrogen bonding in the crystalline surface. NH_3^+ asymmetric and symmetric deformations wavenumbers are expected to fall in the regions $1660\text{--}1610\text{ cm}^{-1}$ and $1550\text{--}1485\text{ cm}^{-1}$ respectively [26]. NH_3^+ deformation is observed at 1614 cm^{-1} in Raman spectrum. This corresponding calculated wavenumber is assigned at 1620 cm^{-1} with 62% PED.

3.2.4 Methine and Methyl group vibrations—

Methyl asymmetric C-H stretching generally falls between at $2972\text{--}2952\text{ cm}^{-1}$, symmetric stretching expected at $2882\text{--}2862\text{ cm}^{-1}$ [24]. CH_3 asymmetric stretching vibrations observed at 2981 cm^{-1} as a medium band in IR and 2979 cm^{-1} as a strong band in Raman. A symmetric stretching vibration of CH is observed as a medium band in both at 2889 cm^{-1} and 2884 cm^{-1} in IR, Raman respectively. Methyl scissoring vibrations appears as a very most intense band at 1440 cm^{-1} (calculated at 1449 cm^{-1}) in Raman. The methyl out-of-plane deformations are assigned at 1374 cm^{-1} (wagging) with 27% PED. CCH deformation is observed at 1177 cm^{-1} in Raman. The $-CH-(CH_3)_2$ group Umbrella modes theoretically assigned at $2944, 2932\text{ cm}^{-1}$. Methine stretching vibrations is observed at 2923 cm^{-1} in Raman spectrum.

3.2.5 Skeletal mode vibrations

The C-N, C-C vibrations bands are generally appears in the region between $1150\text{--}850\text{ cm}^{-1}$ [27,28]. A weak band is observed at 1034 cm^{-1} (IR) and 1036 cm^{-1} (Raman) as attributed to CC stretching vibrations. Combination of C-N and C-C stretching vibrations is observed at 949 cm^{-1} and 947 cm^{-1} in IR and Raman respectively.

3.2.6 Hydrogen bonding vibrations

The attractive interaction between the hydrogen donor group and the acceptor moiety leads to the occurrence of new vibrational degrees of freedom, the so-called hydrogen bond modes. Such modes are connected with elongations changing the A-H \cdots B distance and/or the relative orientations of the hydrogen-bonded groups. This mode occurs at between $50\text{--}300\text{ cm}^{-1}$ [29]. A strong band is observed at 87 cm^{-1} and 120 cm^{-1} (weak shoulder) in Raman which is corresponds to N \cdots O stretching vibration. The computed wavenumbers to the corresponding modes to be assigned at 89 cm^{-1} (55% PED) and 120 cm^{-1} (15% PED).

3.3 NLO properties of DL-Valinium trifluoroacetate

The hyperpolarizability and HOMO-LUMO energy gap was calculated at the B3LYP/6-31G(d,p) level basis set. The frontier orbital electron densities of atoms provide a useful means for the detailed characterization of donor-acceptor interaction [30]. The calculated the first order hyperpolarizability (β) and Energy gap values of LVTFA crystal are given in Table 3. The computed β value (6.42×10^{-30} e.s.u.) of LVTFA crystal is greater than the parent compounds; it is explains their acid-base hybrid crystals hydrogen bonds play an important role not only in the creation of crystal structure and its stability, but also in the enhancement of second order susceptibility of the crystal due to the perturbation of the electronic structure of the organic partner and also due to the strong electron-phonon coupling [31,32,33]. The HOMO orbital energy mainly occupy on Valinium cation moiety and LUMO orbital energy occupy on trifluoroacetate anion moiety. The HOMO and LUMO orbitals are shown in Fig. 4. The HOMO-LUMO energy gap is found to be 6.9 eV.

Table 3: Hyperpolarizability and HOMO-LUMO energy gap values of LVFA crystal

Molecule	Hyperpolarizability (e.s.u.)	HOMO-LUMO Energy Gap
DL-Valinium trifluoroacetate	6.42×10^{-30}	6.9 eV
DL-Valinine	5.72×10^{-30}	6.58 eV
Trifluoroacetic acid	9.29×10^{-31}	5.15 eV

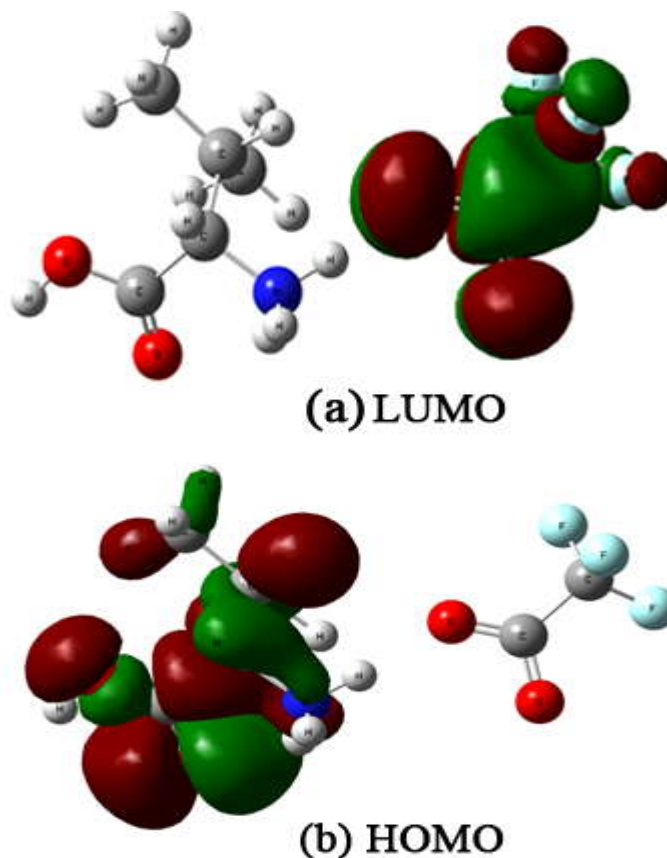


Fig. 4. HOMO, LUMO plots of DL-Valinium trifluoroacetate

4 Conclusions

FT-IR and FT-Raman spectra of the DL-Valinium trifluoroacetate have been recorded and analyzed. Density functional theory calculations at the B3LYP/6-31G(d,p) level basis set has been used to the optimized geometry and vibrational spectra. The vibrational analysis were assigned on the basis of PED analysis and analyzed by using VEDA program. The observed vibrational wavenumbers and optimized geometric parameters were seen to be in good agreement with the experimental data. Optimized geometry, vibrational spectral analysis confirms the presence of N-H \cdots O and O-H \cdots O hydrogen bonding in the crystal. The inverse relationship between first order hyperpolarizability and HOMO-LUMO energy gap has been observed, which allows the molecular orbitals to overlap enabling this VLTF crystal to be an NLO active material.

References

1. Gunter P (Eds.), *Nonlinear Optical Effects and Materials*, (Springer-Verlag, New York), 2000.
2. Aruna S, Anuradha A, Thomas P C, Gulam Mohamed M, Raasekar S A, Vimalan M, Mani G, Sagayaraj P, *Indian J Pure & Appl Phys*, 45(2007)524.
3. Tapati Mallik, Tanusree Kar, *J Cryst Growth*, 274(2005) 251.
4. Petrosyan A M, *Vib Spectrosc*, 41(2006) 97.
5. Pattanaboonmee N, Ramasamy P, Yimmirun R, Manyum P, *J Cryst Growth*, 314(2011) 196.
6. Pandiarajan S, B Sridhar, R K Rajaram, *Acta Crystallogr. E*, 57(2001)466.
7. Sun Z H, L Zhang, D Xu, X Q Wang, X J Liu, G H Zhang, *Spectrochim. Acta A*, 71(2008)663.
8. Srinivasan P, Kanagasekaran T and Gopalakrishnan R, *Cryst. Growth Des.*, 8(2008)2340.
9. Soma A, Tanusree Kar, *J Crystal Growth*, 356(2012)4.
10. Pandiarajan S, Umadevi M, Rajaram R K, Ramakrishnan V, *Spectrochim Acta A*, 62(2005)630.
11. Briget Mary, Umadevi M, Pandiarajan S, Ramakrishnan V, *Spectrochim Acta A*, 60(2004) 2643.
12. Petrosyan A M, *Vibrational Spectroscopy*, 41(2006) 97.
13. Suresh J and Natarajan S, *Acta Cryst. E*, 62(2006) 3331.
14. Becke A. D, *Phys. Rev. A*, 38(1988) 3098.
15. Lee C, Yang W, Parr R.G, *Phys. Rev. B*, 37(1988) 785.
16. Frisch, M. J.; Trucks, G. W.; Schlegel, H. B.; Scuseria, G. E.; Robb, M. A.; Cheeseman, J. R.; Scalmani, G.; Barone, V.; Mennucci, B.; Petersson, G. A.; Nakatsuji, H.; Caricato, M.; Li, X.; Hratchian, H. P.; Izmaylov, A. F.; Bloino, J.; Zheng, G.; Sonnenberg, J. L.; Hada, M.; Ehara, M.; Toyota, K.; Fukuda, R.; Hasegawa, J.; Ishida, M.; Nakajima, T.; Honda, Y.; Kitao, O.; Nakai, H.; Vreven, T.; Montgomery, Jr., J. A.; Peralta, J. E.; Ogliaro, F.; Bearpark, M.; Heyd, J. J.; Brothers, E.; Kudin, K. N.; Staroverov, V. N.; Kobayashi, R.; Normand, J.; Raghavachari, K.; Rendell, A.; Burant, J. C.; Iyengar, S. S.; Tomasi, J.; Cossi, M.; Rega, N.; Millam, J. M.; Klene, M.; Knox, J. E.; Cross, J. B.; Bakken, V.; Adamo, C.; Jaramillo, J.; Gomperts, R.; Stratmann, R. E.; Yazyev, O.; Austin, A. J.; Cammi, R.; Pomelli, C.; Ochterski, J. W.; Martin, R. L.; Morokuma, K.; Zakrzewski, V. G.; Voth, G. A.; Salvador, P.; Dannenberg, J. J.; Dapprich, S.; Daniels, A. D.; Farkas, Ö.; Foresman, J. B.; Ortiz, J. V.; Cioslowski, J.; Fox, D. J. *Gaussian 09*, Revision A.1, Gaussian, Inc., Wallingford CT, 2009.
17. Scott A P, Radom L, *J Phys Chem*, 100(1996)16502.
18. Keresztury G, Holly S, Besenyi G, Varga J, Wang A, Durig J R, *Spectrochim Acta*, A49(1993)2007.
19. Keresztury G, Chalmers J M., Griffith P R (Eds.), *Raman Spectroscopy: Theory, in Hand book of Vibrational Spectroscopy*, (John Wiley and Sons Ltd., New York) 2002.
20. Bellamy L J, *Advance in Infrared Group Frequencies*, (Methuen Publisher), 1968.
21. Gonzalez-Sanchez F, *Spectrochim. Acta A*, 12(1958)17.
22. Lin-Vien D, Colthup N B, Fateley W G, Grasselli J G, *The Handbook of Infrared and Raman Characteristic Frequencies of Organic Molecules*, (Academic Press-London), 1991.
23. Hadzi D and Sheppard N, *Proc. Roy. Soc. Ser. A*, 216(1953) 247.
24. Smith B, *Infrared Spectral Interpretation: A Systematic approach*, (CRC Press, New York) 1998.
25. Socrates G, *Infrared Characteristic Group Frequencies*, (John-Wiley & Sons, New York) 1980.
26. Silverstein R M, Webster F X, *Spectrometric Identification of Organic Compounds*, (Wiley, New York) 1998.
27. Alabugin V, Manoharan M, Peabody S, Weinhold F, *J Am Chem Soc*, 125(2003)5973.

28. Bellamy L J, *The Infra-red Spectra of Complex Molecules*, (Chapman and Hall: London), 1975.
29. Nibbering E T J, Elsaesser T, *Chem Soc Rev*, 104(2004) 1887.
30. Katritzky A R, Lobanov V S, Karelson M, *Chem Soc Rev*, 24(1995)279.
31. Shen Y, *The Principles of Nonlinear Optics*, (Wiley, New York) 1984.
32. Bishop D M, Kirtman B, Champagne B, *J Phys Chem A*, 101(1997)5780.
33. Vijayakumar T, Hubert Joe I, Reghunadhan Nair C P, Jayakumar V S, *J Mol Struct*, 877(2008)20.